Utilizing of (nTiO$_2$) Nanoparticles in Thin Films Based on Polystyrene Blending with (DCM) Laser Dye

Ahmed Namah Mohamed, M. F. Jaddoa, and Akeel Shaker Tuhaiwer

Department of Physics,
College of Science,
University of Al-Muthanna,
Samawa, Iraq

Titania nanoparticles (nTiO$_2$) are synthesized by sol–gel technique. Characterization of nTiO$_2$ is accomplished with XRD instrument. SEM is used to analyse the structure of nTiO$_2$ samples and to determine nanoparticle sizes. Various concentrations of nTiO$_2$ (0.5, 1, 1.5, 2 and 2.5 ml) blended with DCM laser dye blended with polymer (polystyrene) are synthesized *via* casting technique. Investigations of the effect of these additions on both optical properties and electronic-transition energy gaps in cases of Tauc's model and derivative absorption spectra are carried out. The results of the allowed direct electronic transition energy gap indicate decreasing from 2.3 to 2.23 eV as nTiO$_2$ concentration increase, whereas the energy gap magnitudes found from the first absorbance derivative decrease from 2.348 to 2.313 eV as nTiO$_2$ concentration increase.

Наночастинки діоксиду титану (nTiO$_2$) синтезовано за допомогою золь-ґель-методики. Характеризацію nTiO$_2$ виконано за допомогою рентґенівського дифракційного інструментарію. Сканувальну електронну мікроскопію використано для аналізи структури зразків nTiO$_2$ та визначення розмірів наночастинок. Різні концентрації nTiO$_2$ (0,5, 1, 1,5, 2 і 2,5 мл) у суміші з лазерним барвником 4-(dicyanomethylene)-2-methyl-6-(p-dimethylaminostyryl)-4H-pyran, змішаним з полімером (полістиролом), синтезовано за допомогою методи лиття. Проведено дослідження впливу цих присадок як на оптичні властивості, так і на електронні перехідні енергетичні щілини у випадках моделю Таука та похідних спектрів поглинання. Результати дозволеної прямої електронної перехідної енергетичної щілини свідчать про пониження з 2,3 до 2,23 еВ у міру збільшення концентрації nTiO$_2$, тоді як величини енергетичної щілини, виявлені за першою похідною абсорбції, зменшуються з 2,348 до 2,313 еВ у міру збільшення концентрації nTiO$_2$.

Key words: optical absorption, titania nanoparticles (nTiO$_2$), first absorbance

1. INTRODUCTION

Extensive research contributions have been done to improve amorphous polymeric materials with a high ionic conductivity at room temperature besides good mechanical, optical, and thermal characteristics [1]. Doping of polymers had attracted more interest by scientists and technicians because of their wide applications. The blend in polymer can change the polymer structure and hence the microstructural characteristics of the polymer [2]. One of the techniques that are used to obtain amorphous kind of electrolyte is based on dissolving the salt in the immobilized polymer matrix. Moreover, this polymer is considered as an excellent host matter for various composites. Different research groups are examining the obvious trace of blending on all optical, thermal, structural, and mechanical characteristics [3]. The polymer optical characterizations can be enhancing by addition of blends to be dependent on their reactivity with the host matrix. Many researchers have examined the properties of acid-based polymer electrolyte complexes such as proton conductors and their potential usages in solid-state devices [4]. Polystyrene (PS) is one of unique polymeric material, which has wide applications in industry and its relatively low cost [5]. PS is a potential matter, which exhibits a higher dielectric strength, better capacity for storage of the charges, and improve optical and electrical characterizations for dopants [6]. Recent researches show the water molecules inside the PS-based electrolyte enhanced the conductivity while it preserved the dimensional stability of the electrolyte [7].

Titanium dioxide (TiO$_2$) has energy gap of (3.2 eV) for n-type semiconductor with variety important properties such as a high refractive index, low absorption coefficient in visible light, and good chemical stability [8]. Recently, nanocomposite semiconductors get more interests comparing with traditional semiconductor materials due to its unique advantages such as cheap manufacturing, easy techniques used to prepare, a large variety of applications, and very suitable candidate for substrate choice [9]. TiO$_2$ nanoparticles have been widely used as dye-sensitized solar cells (DSSCs) [10], gas sensor [11], and UV sensor [12]. UV sensors can be used as sensors in almost chemical and environmental detecting applications such as emitter calibration, analysis of chemical and biological samples, telecommunications, flame detection, and atmospheric and space studies [13]. TiO$_2$ nanoparticles have a

high sensitivity to UV light, and much higher surface-area-to-volume ratio can enhance the total photoreactivity [14]. Some researches reveal that the salts are excellent proton donors to the polymer matrix, and salts blended with PS are rare. In the present work, the preparation and properties of polymer electrolytes based on polystyrene blended with DCM laser dye and (nTiO$_2$) nanoparticles have been studied. Tetrahydrofuran (THF) was used in this process as a solvent.

Absorbance (A) is measured using UV−VIS dual beam spectrophotometer, which has a range of wavelengths of 190−1100 nm. The absorption coefficient (α) was calculated using relation (1) [15]:

$$\alpha = \frac{2.303A}{x},\tag{1}$$

where x is the film thickness.

The absorption coefficient is a crucial parameter because it supplies specific data about the electronic transition by using Eq. (2) [16]:

$$\alpha = B\frac{(h\nu - E_g)^{1/2}}{h\nu},\tag{2}$$

where B is constant, and ν is frequency.

The absorption spectra measurement (and particularly the peak of absorption curve) is a good tool to investigate the optical behaviour of prompted transitions and provides significant data about the configuration and optical energy gap in thin films. The absorption edge in different composites follows the known Urbach's rule as in the following Eq. (3) [17]:

$$\alpha = \alpha_o\exp\left(\frac{h\nu}{E_u}\right).\tag{3}$$

The extinction coefficient (K) can be expressed in terms of the absorption coefficient as Eq. (4) [18]:

$$K = \frac{\lambda\alpha}{4\pi}.\tag{4}$$

The refractive index (n) can be calculated using Eq. (5) [19]:

$$n = \frac{1 + \sqrt{R}}{1 - \sqrt{R}}.\tag{5}$$

In order to determine refractive index for dispersion of DCM−PS blend with nTiO$_2$ nanoparticles in thin films at various annealing temperatures, the single-oscillator model developed by DiDomenico and Wemple is considered [20]. The refractive index can be expressed in

terms of the dispersion energy E_d and single-oscillator energy E_o according to Eq. (6):

$$n^2 = 1 + \frac{E_d E_o}{E_o^2 - (h\nu)^2} .$$ (6)

2. EXPERIMENTAL PART

The adjustment amount of DCM dye was dissolved in alcohol (in our experiment, it was $5 \cdot 10^{-3}$ mole/litre) to get the suitable concentration of laser dye solutions. Sol–gel method was used to manufacture titanium dioxide nanoparticles with 10 ml of titanium alkoxide as a raw material mixed with 40 ml of 2-propanol in a dry atmosphere. This mixture was then added drop wise into another mixture, which consists of 10 ml water and 10 ml of 2-propanol. One hour of stirring, transparent gel with yellow colour is produced. The prepared gel was subsequently dried at temperature 105°C for several hours until totally turned into a yellow block structure. The examined materials are calculated by putting it at 500°C for six hours in a furnace.

The nanopowder structure was investigated with a Shimadzu 6000 x-ray diffractometer using CuK_α radiation ($\lambda = 1.5406$ Å). The morphology of $nTiO_2$ samples is achieved *via* a scanning electron microscopy (SEM) in order to control the size of nanoparticles.

To prepare PS blend with DCM thin films, firstly, 0.015 gm from DCM dissolved in 10 ml of tetrahydrofuran (THF) solvent and stirrer for around 30 minutes to obtain homogenous solution; then, 2 gm PS dissolve in 30 ml THF and stirring for 2 hours to obtain the polymer solution. To synthesize the final thin films, 1 ml DCM solution was mixed with 5 ml PS solution and *in situ* casting on glass substrate at a room temperature. Various concentrations of obtained $nTiO_2$ nanoparticles (0.5, 1, 1.5, 2, and 2.5 ml) were suspended separately one by one into THF solvent and added to the mixture of DCM–PS. The final prepared films were marked as (*A*, *B*, *C*, *D*, and *E*) as the nanoparticles concentration increased.

The thickness of prepared thin films was measured by using the optical interferometer process with employing He–Ne laser of 0.632 μm. The thickness was roughly of 0.45 um for all samples.

3. RESULTS AND DISCUSSION

The scanning electron microscopy (SEM) image of $nTiO_2$ nanoparticles is shown in Fig. 1.

Determination of titania particle size was carried out with (SEM) pattern after preparing $nTiO_2$ at pH3 and 500°C calcination tempera-
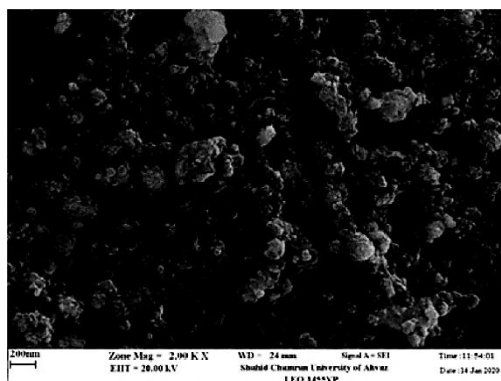
Fig. 1. Scanning electron microscopy of the nTiO$_2$ nanoparticles.
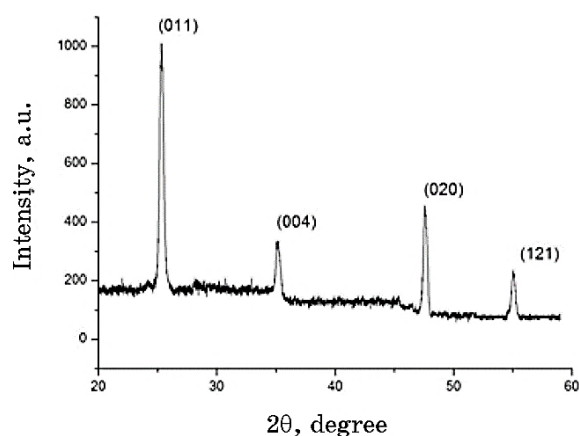
Fig. 2. XRD pattern of the nTiO$_2$ nanoparticles.

ture; the prepared nanoparticles are suspended as film using spin coating process. The achievement value of nTiO$_2$ nanoparticles' size is about of 55.82 nm.

In addition, the XRD pattern of the nTiO$_2$ nanoparticles, which were synthesized *via* sol−gel technique at pH3 and calcination of the synthesized material accomplished at temperature of 500°C for 6 hours in furnace, is shown in Fig. 2.

The anatase phase was identified at 2θ of 25.40°, 38.10°, 48.20°, 53.90°, and 55.10°. The characteristic peak of anatase is sharp and clear to observe, in particular, at 25.40° degree.

The absorption spectra for PS doping with DCM and nTiO$_2$ nanoparticles' thin films at room temperature is illustrated in Fig. 3.

It can be seen that, for PS blending with DCM and nTiO$_2$ nanoparticles' thin films, the intensity of absorption band is increased with in-
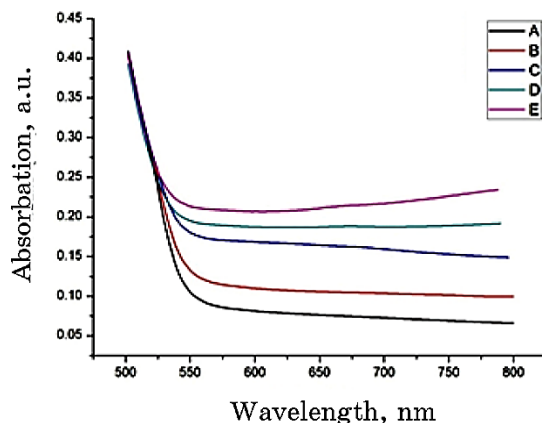
Fig. 3. Absorbance for PS blend with DCM thin films filled with various concentrations of titania nanoparticles.
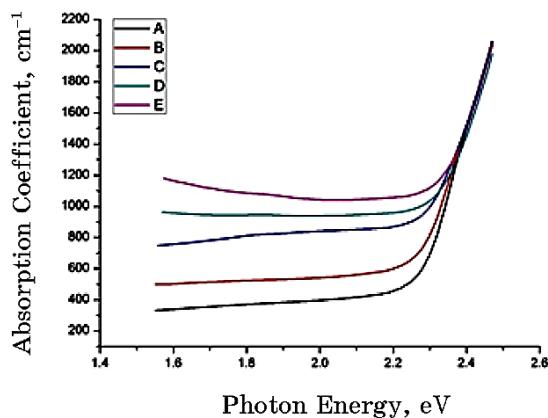
Fig. 4. Absorption coefficient for PS blend with DCM thin films filled with various concentrations of titania nanoparticles.

creasing nTiO$_2$ nanoparticles' concentration as shown in Fig. 3. The reason of these variations is due to increasing of concentration of nTiO$_2$ nanoparticles, which causes increasing the number of molecules in volume unit that leads to change in energy level of nTiO$_2$ nanoparticles as a result of increasing in perturbation field on the molecules; this agree with the explanation of Tsiaousis and Munn (2002) [21].

Figure 4 shows the absorption coefficient trend as a function of photon energy for PS blend with DCM thin films filled with various concentrations of titania nanoparticles. Absorption coefficient is determined from absorbance measurements using Eq. (1).

The absorption coefficient of PS blend with DCM thin films filled with
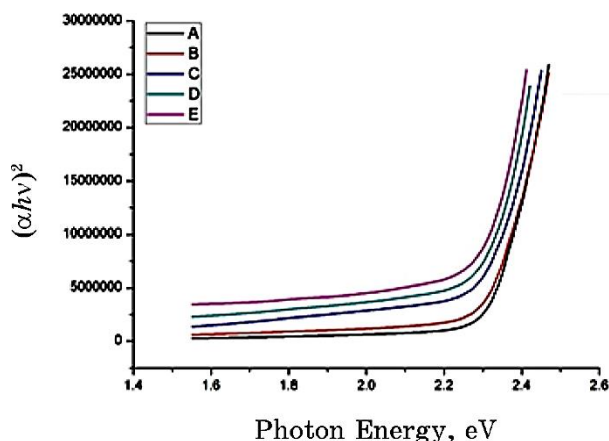
Fig. 5. Relationship between $(\alpha h\nu)^2$ and photon energy (eV) for PS blend with DCM thin films filled with various concentrations of titania nanoparticles.

various concentrations of titania nanoparticles decreased in the end of visible region because it is inversely proportional to the reflectance. This can be linked with increase in grain size, and it may be attributed to the light scattering effect for its high surface roughness [22].

The energy gaps (E_g) of PS blend with DCM thin films filled with various concentrations of titania nanoparticles were evaluated from the absorption spectra, and the optical absorption coefficient (α) near the absorption edge for allowed direct transitions is given by Eq. (2).

The characteristics of $(\alpha h\nu)^2$ *vs.* photon energy are plotted for evaluating the band gap (E_g) of PS blend with DCM thin films filled with various concentrations of titania nanoparticles, and extrapolating the linear portion near the onset of absorption edge to the energy axis as shown in Fig. 5.

As can be seen clearly, E_g of PS blend with DCM filled thin films has various values of 2.3, 2.285, 2.26, 2.25, and 2.23 eV corresponding to nTiO$_2$ concentrations of 0.5, 1, 1.5, 2, and 2.5, respectively, as shown in Table. In other words, the band gaps of films become tight as nTiO$_2$ content increases, where titania nanoparticles' concentration will produce more localized levels close to the structure valence and conduction band that leads to gather electrons and generate tails lowering the optical energy gap, which is consistent with [23].

Figure 6 indicates the effect of the first absorption derivative on the photon energy for all thin films.

The spectra obviously show that the increase concentration of prepared titania declined the energy gap for all samples. Table lists the energy gap values, which are obtained from the first derivative; this is identical with the results of Tauc's model of the energy band gap val-
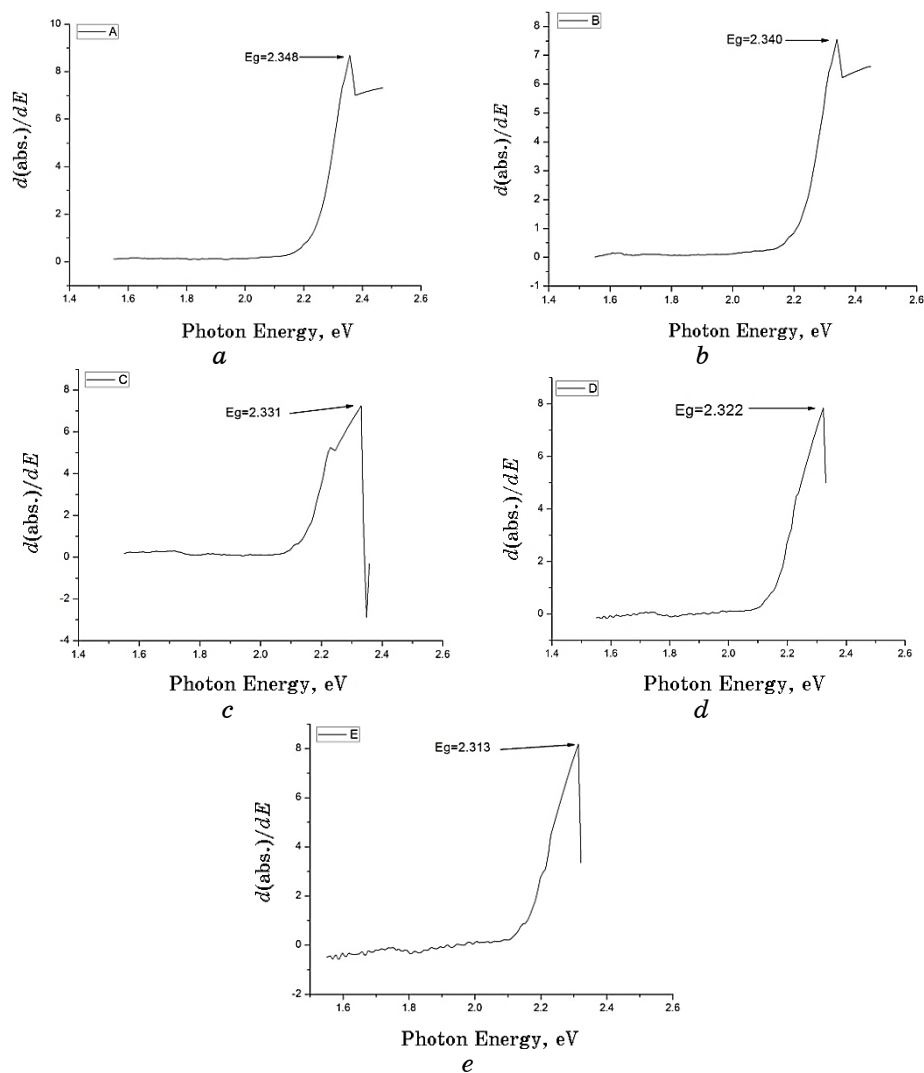
Fig. 6. Relationship between the absorption and photon energy.

ues, which are agree with [24].

The Urbach's energy magnitudes were calculated by taking inverted incline of the straight line of the curve. Moreover, Figure 7 shows the relation of $\ln\alpha$ *vs.* photon energy (eV) for DCM−PS blend with nTiO$_2$ nanoparticles' thin films. Urbach's energy values are indexed in Table.

Urbach's energy values were rising with grows up of tiny particle density of titania because the sum of localized energy levels in the optical energy gap had increased and caused an increase of the tails of Urbach's energy. These changes lead to a decrease in the optical energy

TABLE. The calculated parameters for examined mixtures.

Sample	Concentration of titania nanoparticles, ml	Single-oscillator energy E_o, eV	Dispersion energy E_d, eV	Urbach's energy E_U, eV	E_g, eV, from Tauc's model	E_g, eV, from derivative absorption spectra
A	0.5	5.097	4.920	2.106	2.3	2.348
B	1	4.689	4.822	2.468	2.285	2.340
C	1.5	4.611	4.669	2.788	2.26	2.331
D	2	4.354	4.638	2.840	2.25	2.322
E	2.5	4.191	4.469	2.981	2.23	2.313
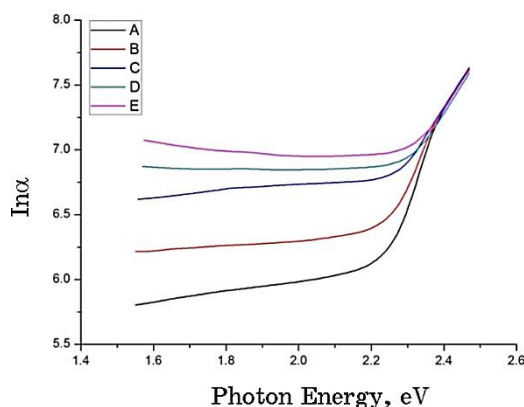
Fig. 7. Urbach's energy as a function of photon energy (eV) for prepared films.

gap. This means that the optical attitude of the energy value of Urbach's tails is conflicting to the optical trend of the optical energy gap, and thus, the structure turns into well-crystallized one [25].

Extinction coefficient (K) is correlating with the absorption of light and then related to absorption coefficient by the Eq. (4). Therefore, K can be measured using the previous relation. The curves of extinction coefficient for PS blend with DCM thin films are shown in Fig. 8.

Extinction coefficient and absorption coefficient behave similarly because both they are joined by previous relation, and extinction coefficient increasing with increasing of concentration.

Reflectance spectra for prepared thin films were investigated at room temperature and presented in Fig. 9.
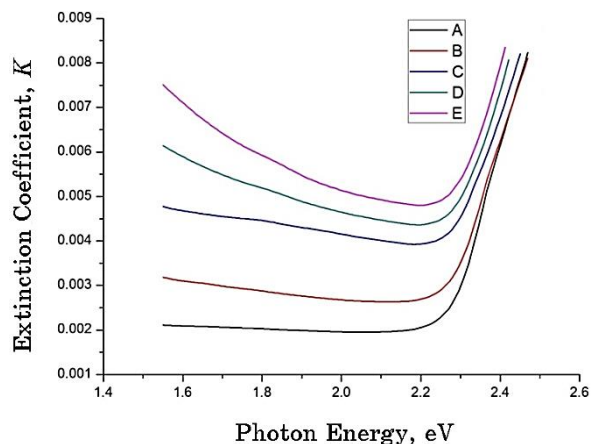
Fig. 8. Extinction coefficient *vs.* photon energy.
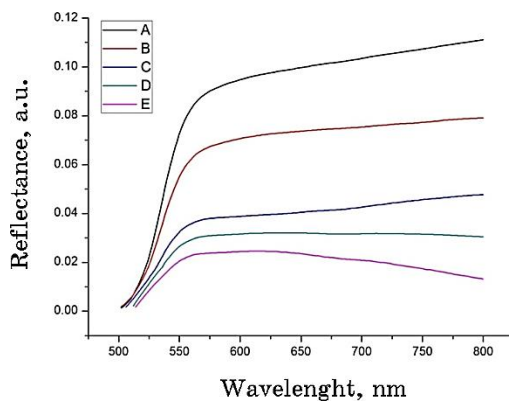
Fig. 9. Reflectance curves for all samples.

The reflectance plots indicate that the rise in nanoparticles' concentration causes the decline in reflection intensity; it was assumed that the existence of (nTiO$_2$) nanoparticles in starch-based polymer highly enhanced the UV-resistance ability of the polymer.

The refractive indices of prepared films are determined from Eq. (5). Figure 10 shows the variation in refractive index with energy for various nTiO$_2$ nanoparticles' concentration.

This trend shows an increase of the value of refractive index with higher concentration. The increase may be resulted from higher packing concentration of the films and, hence, caused change in the refractive index.

The relation $1/(n^2-1)$ *vs.* $(h\nu)^2$ is plotted in Fig. 11, and from the curves, it can be determined the single-oscillator energy (E_o) and dis-
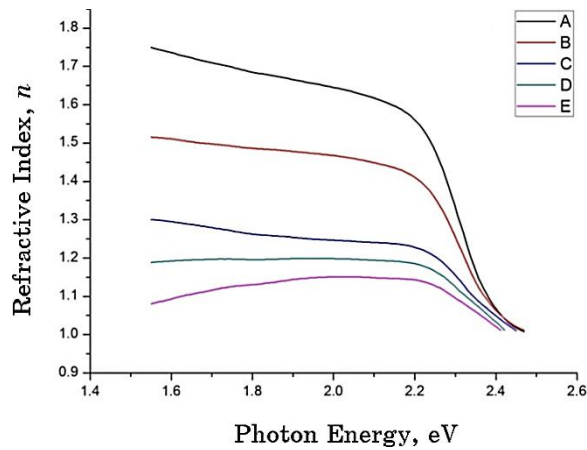
Fig. 10. The relation between refractive index and energy at various concentrations.
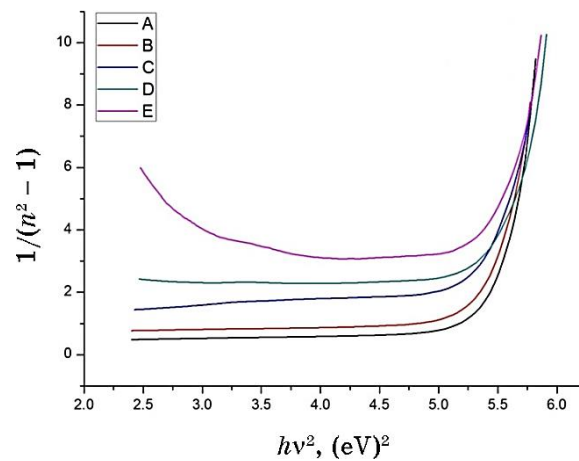
Fig. 11. Relationship between $1/(n^2 - 1)$ and $(h\nu)^2$ for various concentrations' samples.

persion energy (E_d) values. E_o is an average energy gap and can be related to the band gap, E_g, in close approximation $E_o \approx 2E_g$ [26].

The values of E_o and E_d were calculated from the slope and intercept on the vertical axis of $1/(n^2 - 1)$ $vs.$ $(h\nu)^2$ plot; they are listed in Table.

4. CONCLUSION

In this work, titania nanoparticles (nTiO$_2$) were synthesized via sol−gel technique. Various (nTiO$_2$) concentrations are co-doping with (DCM)

laser dye blend with polystyrene (PS) and prepared using casting method. The effect of addition of various (nTiO$_2$) concentrations on the optical properties is studied and investigated by using UV−VIS spectrometer. Increases of (nTiO$_2$) concentrations for all films cause decreasing in the direct electronic transitions in magnitude of 2.3−2.23 eV. The energy gap from derivative absorption spectra was 2.348−2.313 eV. This decreasing also affects to decrease in the refractive index values, the single-oscillator energy (E_o) and dispersion energy (E_d). Whereas, it causes increasing in extinction coefficient and absorption coefficient for all fabricated films. In addition, Urbach's tail assures that the crosslink is increased as the titania nanoparticles' densities increase: 2.106−2.981 eV.

REFERENCES

1. S. S. Chiad, B. H. Abed, and N. F. Habubi, *Iraqi Journal of Physics*, **10**, No. 17: 18 (2012).
2. G. Hirankumar, S. Selvasekarapandian, N. Kuwata, J. Kawamura, and T. Hattori, *Journal of Power Sources*, **144**, No. 1: 262 (2005).
3. M. Abdelaziz and M. M. Ghannam, *Physica B: Condensed Matter*, **405**, No. 3: 958 (2010).
4. M. Kaseem and Y. G. Ko, *Journal of Polymers and the Environment*, **25**, No. 4: 994 (2017).
5. M. Krumova, D. Lopez, R. Benavente, C. Mijangos, and J. M. Perena, *Polymer*, **41**, No. 26: 9265 (2000).
6. R. A. Vargas, V. H. Zapata, E. Matallana, and M. A. Vargas, *Electrochimica Acta*, **46**, Nos. 10−11: 1699 (2001).
7. M. A. Vargas, R. A. Vargas, and B. E. Mellander, *Electrochimica Acta*, **45**, Nos. 8−9: 1399 (2000).
8. E. Khalili Dermani, *Sciences*, **38**, No. 1: 19 (2014).
9. G. Konstantatos and E. H. Sargent, *Proceedings of the IEEE*, **97**, No. 10: 1666 (2009).
10. X. Xin, M. Scheiner, M. Ye, and Z. Lin, *Langmuir*, **27**, No. 23: 14594 (2011).
11. M. Gholami, M. Bahar, and M. E. Azim-Araghi, *Chem. Phys. Lett*, **48**: 9626 (2012).
12. N. H. Kargan, M. Aliahmad, and S. Azizi, *Soft Nanoscience Letters*, **2**: 29 (2012).
13. U. M. Nayef, K. A. Hubeatir, and Z. J. Abdulkareem, *Optik*, **127**, No. 5: 2806 (2016).
14. S. I. Alnassar, E. Akman, B. G. Oztoprak, E. Kacar, O. Gundogdu, A. Khaleel, and A. Demir, *Optics & Laser Technology*, **51**: 17 (2013).
15. A. S. Tuhaiwer, *Almuthanna Journal of Pure Science (MJPS)*, **5**, No. 1: (2018).
16. F. Ahmad and E. Sheha, *Journal of Advanced Research*, **4**, No. 2: 155 (2013).
17. N. F. Habubi, *Al-Mustansiriyah Journal of Science*, **21**, No. 5: 41 (2010).
18. T. S. Girisun and S. Dhanuskodi, *Crystal Research and Technology: Journal of Experimental and Industrial Crystallography*, **44**, No. 12: 1297 (2009).
19. M. K. Dhahir and R. A. Faris, *Iraqi Journal of Laser*, **15A**: 9 (2016).

20. N. F. Habubi, N. A. Bakr, and S. A. Salman, *PCAIJ*, **8**, No. 2: 54 (2013).
21. D. Tsiaousis and R. W. Munn, *The Journal of Chemical Physics*, **117**, No. 23: 10860 (2002).
22. S. Karvinen, *Solid State Sciences*, **5**, No. 5: 811 (2003).
23. S. S. Chiad, *International Letters of Chemistry, Physics and Astronomy*, **45**: 51 (2015).
24. A. E. Morales, E. S. Mora, and U. Pal, *Revista Mexicana de Física*, **53**, No. 5: 18 (2007).
25. M. H. Abdul-Allah, N. F. Habubi, and S. S. Chiad, *Iraqi Journal of Physics*, **10**, No. 17: 12 (2012).
26. A. H. Ammar, A. M. Farid, A. A. M. Farag, K. A. A. Sharshar, F. S. H. Abu-Samaha, and K. M. Hamad, *Journal of Non-Crystalline Solids*, **416**: 50 (2015).